https://doi.org/10.5194/essd-2022-123
Preprint. Discussion started: 1 July 2022

Open Access Earth System Science Data Discussions

Pan-Arctic soil element availability estimations

Peter Stimmler[1], Mathias Goeckede[2], Bo Elberling[3], Susan Natali[4], Peter Kuhry[5], Nia Perron[6], Fabrice Lacroix[2], Gustaf Hugelius[5,7], Oliver Sonnentag[6], Jens Strauss[8], Christina Minions[4], Michael Sommer[1], and Jörg Schaller[1*]

[1] Leibniz Centre for Agricultural Landscape Research (ZALF), Müncheberg, Germany
[2] Max Planck Institute for Biogeochemistry, Jena, Germany
[3] Center for Permafrost, Department of Geosciences and Natural Resource Management, University of Copenhagen, Copenhagen, Denmark
[4] Woodwell Climate Research Center, Falmouth, USA
[5] University Stockholm, Stockholm, Sweden
[6] Département de Géographie, Université de Montréal, 1375 Avenue Thérèse-Lavoie-Roux, Montréal, QC H2V 0B3, Canada
[7] Bolin Centre for Climate Research, Stockholm University, Stockholm, Sweden
[8] Alfred Wegener Institute Helmholtz Centre for Polar and Marine Research, Permafrost Research Section, Potsdam, Germany

** Correspondence to: email: Joerg.Schaller@zalf.de*

Abstract. Arctic soils store large amounts of organic carbon and other elements such as amorphous silica, silicon, calcium, iron, aluminium, and phosphorous. Global warming is projected to be most pronounced in the Arctic leading to thawing permafrost, which in turn is changing the soil element availability. To project how biogeochemical cycling in Arctic ecosystems will be affected by climate change, there is a need for data on element availability. Here, we analysed amorphous silica (ASi), silicon (Si), calcium (Ca), iron (Fe), phosphorus (P), and aluminium (Al) availability from 574 soil samples from the circumpolar Arctic region. We show large differences in ASi, Si, Ca, Fe, P, and Al availability among different lithologies and Arctic regions. We summarized these data in pan-Arctic maps of ASi, Si, Ca, Fe, P, and Al concentrations focussing on the top 100 cm of Arctic soil. Furthermore, we provide values for element availability for the organic and the mineral layer of the seasonally thawing active layer as well as for the uppermost permafrost layer. Our spatially explicit data on differences in the availability of elements between the different lithological classes and regions now and in the future will improve Arctic Earth system models for estimating current and future carbon and nutrient feedbacks under climate change.

https://doi.org/10.5194/essd-2022-123
Preprint. Discussion started: 1 July 2022

Open Access Earth System Science Data Discussions

1 Introduction

Temperatures in northern high latitude region have risen more than twice as fast as the global average within the last decades (IPCC, 2021). This warming leads to thawing of perennially frozen ground known as permafrost (Brown and Romanovsky, 2008; Romanovsky et al., 2010). Frozen conditions prevent organic matter (OM) from microbial degradation and also limits fluvial export of soil-bound nutrients to the sea by runoff (Mann et al., 2022). Thawing of frozen ground (defined as permafrost soils in the following) may in turn accelerate global warming by potentially releasing potent greenhouse gases such as carbon dioxide (CO2) and methane (CH4) through soil organic carbon mineralization (Schuur et al., 2015). The frozen ground of the Arctic-boreal regions (hereafter called 'Arctic', but also including subarctic regions) are the largest pool of soil organic carbon worldwide. Approximately, 1014 - 1035 ± max. 194 Pg of organic carbon is stored within the upper 3 m of permafrost region soils (Hugelius et al., 2014; Mishra et al., 2021). To full depth, ca. 1460 - 1600 Pg carbon is stored in the permafrost region (Strauss et al., 2021a), and approximately one third of this is in ice rich Yedoma deposits, exceeding 3m depth (Fuchs et al., 2018; Strauss et al., 2017). The Yedoma deposits formed in unglaciated areas of the northern hemisphere during the glacial period, when melt water from glacial areas and eolian processes transported fine sediment to the unglaciated lowlands (Schuur et al., 2013; Strauss et al., 2021b; Strauss et al., 2013). Yedoma deposits are characterized by high carbon and water content. The water is mostly bound in massive ice in ice wedges as well as segregated ice and pore ice in sediment columns (Schirrmeister et al., 2011). Thus, Yedoma soils are highly vulnerable to thawing as the loss of the high ice volume leads to surface subsidence and thermokarst processes, which can accelerate thaw and remobilize deep elemental stocks.

The temperature and near-surface water content in the Arctic soils have changed rapidly in the last decades and further changes are expected in future (Box et al., 2019). An important effect of Arctic warming is a deepening of the seasonally-thawed active layer and related thermokarst processes, which may lead to a mobilization of nutrients from permafrost soil layers (Abbott et al., 2015). Additionally, increased temperatures in the Arctic regions may accelerate weathering, potentially enhancing nutrient availability in terrestrial Arctic ecosystems and export to freshwater systems, and finally to the nearshore zone and sea (Holmes et al., 2013).

As the Arctic features a mineral composition of the sediments that is different from many other global soils (Monhonval et al., 2021a), the availability (for microbes and plants) of elements in Arctic soils may differ as well. Yedoma deposits, for example, are important pools of OM in the Arctic. Because Yedoma deposits include materials transported from nearby mountains, the mineral compositions of the Yedoma soils depend on the original geology of the mountains (Schirrmeister et al., 2011). Sediments of marine origin are often rich in calcium (Ca), phosphorus (P) and silicon (Si), while magmatic rocks such as granite or basalt contain large amounts of Si, iron (Fe), aluminum (Al), and P. The availability of these elements in soils is the complex product of soil genesis and nutrient release, which depend on physical and chemical conditions including temperature, water content and pH. In this context, Si, Ca, Fe, Al or P are bound in or on mineral phases and are released via enzymatic activity or weathering. Ongoing Arctic climate warming now threatens to disturb the pools that have equilibrated to conditions characteristic for the past millennia.

https://doi.org/10.5194/essd-2022-123
Preprint. Discussion started: 1 July 2022

The availability of elements such as P, Fe, Ca, and Si in soils are known controls for soil OM respiration (Brady and Weil, 2008; Schaller et al., 2019). A release of inorganic nutrients such as P or Si can lead to increased greenhouse gas production and potentially to further export of this elements to the fresh and seawaters. In marine systems, P, Fe, Ca, and Si are well-known to control carbon (C) fixation in terms of algae biomass productivity (Tremblay et al., 2015). In terrestrial systems, P availability is positively related to silicic acid ($Si(OH)_4$) (Schaller et al., 2019) or its polymers, which mobilize from, e.g., amorphous silica (ASi) (Schaller et al., 2021). The mobilization of P by Si was shown to occur due to competition for binding at Fe-minerals (Schaller et al., 2019), which tend to strongly bind P under condition of low Si availability (Gérard, 2016). Contrary to Si, Ca bind P by calcium phosphate co-precipitation with calcium carbonate, at least under high soil pH conditions (Otsuki and Wetzel, 1972). Like P, OM is also binding to Ca, Fe and Al-phases (Kaiser and Zech, 1997; Wiseman and Püttmann, 2006) but being mobilized from those phases by Si (Hömberg et al., 2020). If the Fe availability in soils is low, the binding of P may be related to Al-minerals (Eriksson et al., 2015).

Despite the important role of soil elements in driving soil and ecosystem processes and the potential for rapid changes in the Arctic due to climate change, the spatial distribution of elemental stocks (beyond C, N) is not well understood. An ecologically based classification of soil Ca concentrations was proposed by Walker et al. (2001), differentiating between a Ca rich non-acidic tundra and a Ca poor acidic tundra based on differences in vegetation types for the Alaskan Arctic region. This classification system was further used to estimate pan-Arctic soil OM stocks (Hugelius et al., 2014), which proved to be a useful approach as vegetation is tightly connected to OM stocks (Quideau et al., 2001). Based on the work of Hugelius et al. (2014), Alfredsson et al. (2016) related vegetation cover to amorphous Si (ASi) concentration to scale up Arctic ASi stocks. However, in contrast to OM stocks being clearly related to vegetation (Hugelius et al., 2014), the effect of vegetation on mineral availability in soils is debatable. Therefore, the extrapolation of circum-polar Arctic maps of element availability for P, Fe, Ca, Al, and Si based on vegetation distribution alone may be associated with high uncertainties. A much stronger driver of element availability could be parent material and lithology (Alloway, 2013).

In this study, we aim to map pan-Arctic soil element bio-availability (for microbes and plants) by applying a lithology-based extrapolation of plot level sampling data on nutrient availability. We provide maps for ASi, Si, Ca, Fe, P and Al as these elements have direct effects on OM binding and greenhouse gas (GHG) emission from the circumpolar Arctic. In addition, these elements are limiting nutrients for CO_2 binding in terms of primary production in Arctic marine systems or interfere with those. Better understanding of element availability is crucial to reduce uncertainties for reliable modelling of future scenarios on how Arctic system may respond to global warming.

https://doi.org/10.5194/essd-2022-123
Preprint. Discussion started: 1 July 2022

2 Material and Methods

2.1 General approach

Based on the Geological Map of the Arctic (Harrison et al., 2011), we estimate the bio-availability and potential mobility of ASi, Si, Ca, Fe, Al and P in Arctic soils. We analyzed soil samples from organic, mineral and permafrost layers from pan-Arctic sampling campaigns. We used the biological available element concentrations of certain lithologies to compile pan-Arctic maps covering 7.6x106 km² for ASi, mineral Si, Ca, Fe, Al and P.

2.2 Sampling and storage

In total, we analyzed 574 Arctic soil samples from 25 locations (Fig. 1). To ensure a pan-Arctic coverage we analyzed samples from Siberia (222 samples from six locations), North America (115 samples from six locations), Greenland (111 samples from nine locations), Northern Europe (13 samples from one location) and Svalbard (103 samples from three locations) (Fig. 1 and S1, Table S1). We analyzed samples from the thawed near-surface organic layer (252 soil samples, mainly 0-20 cm in depth), mineral layer (208 soil samples, mainly 20-50 cm depth)) and permafrost layer (104 soil samples, mainly 50-100 cm depth). We split the annually thawed active layer in the upper organic layer and the mineral layer below by C content, except for soils where the organic layer corresponds to the active layer. The organic layer contained mainly organic matter (OM) in different mineralization states. The mineral soil layer has variable OM content depending on which soil processes have affected this layer and reaches to the perennially frozen permafrost layer. We took samples using an auger or a spade and stored them frozen until analysis or as described before (Faucherre et al., 2018; Kuhry et al., 2020). Samples consisted of 5-50 g frozen soil. Before analysis, the samples were oven dried and ground.

2.3 Extraction and analysis

Available concentrations of Si, Ca, Fe, Al and P were quantified using the Mehlich III method (Sims, 1989). Briefly, we extracted 0.5 to 5 g of freeze-dried soil using 10 ml g-1 Mehlich III solution (0.015 M NH4F, 0.001 M EDTA, 0.25 M NH4NO3, 0.00325 M HNO3, 0.2 M HAc). The samples were shaken for 5 min at 200 min-1 and centrifuged for 5 min at 10.000 x g. Afterwards, the supernatant was filtered using a 0.2 µm cellulose acetate filter. The analysis was done by inductive coupled plasma with optical emission spectroscopy (ICP-OES) (Vista-PRO radial, Varian Medical Systems, Palo Alto, California). For extraction of available amorphous silica (ASi) an alkaline extraction was used (DeMaster 1981), extracting ASi from 30 mg of freeze-dried soil using 40 ml 0.1 M Na2CO3 solution at 85°C for 5 h. After 1 h, 3 h and 5 h the suspension was mixed, and 10 ml of the supernatant was subsampled, filtered by a 0.2 µm cellulose acetate filter and analyzed by ICP-OES. The ASi concentration was calculated using a linear regression of ASi concentration in solution over time and the intersection with the Y-axis was used as concentration of available concentration according to DeMaster (1981). To determine the dry weight (DW) of the samples 0.5-2 g of frozen material was freeze dried until weight constancy.

https://doi.org/10.5194/essd-2022-123
Preprint. Discussion started: 1 July 2022

134 **2.4 Statistics**

135 **2.4.1 Statistics and graphics**

136 Data were analyzed using the R Studio (R_Core_Team, 2021). We extracted the original data (lithology, location,
137 geometry) given for GIS polygons (shape files from the different regions, Greenland, Can_USA, Ice,
138 N_Europa_Russia) of the Geological Map of the Arctic containing locations. We extracted 14 lithological classes in
139 total. We matched the soil sampling locations for which we obtained data for element availability by extraction (see
140 above) with the GIS polygons (geology) by ARCView_GIS_3.2 extensions "Spatial Analyst" command "analysis:
141 tabulate Areas". The sum of areas with the same map label was extracted by map label "shape area". We considered
142 only terrestrial areas. For every location, we calculated the element concentrations for the different samples from
143 organic, mineral and permafrost layer. We calculated quantiles, mean and standard error using "summarise" from the
144 "dplyr" R package. We clustered element concentration data for all locations by lithological class and calculated mean
145 and standard error for organic, mineral and permafrost layer. The number of samples for each lithological class is
146 given in Fig. 1.
147

148 **2.4.2 Element concentration maps**

149 We used the "Geological Map of the Arctic (1:5 000 000 scale, in the Arctic polar region, north of latitude 60°N") as
150 the basis for our maps. We calculated the weighted numeric mean concentration for each element in the first 100 cm
151 from the soil surface using formula (1). The mean mass fraction (wm) of an element (X) is the sum of the products of
152 the mass fractions in organic (OL), mineral (ML) and permafrost (PL) layer and the thickness (d) of each layer in cm
153 divided by 100 cm. We colored the represented area based on the element concentration.

154 $$w_m\,(X)\left[\frac{mg}{g}\right] = \frac{(w_{OL}(X)\left[\frac{mg}{g}\right]*d_{OL}\,[m] + w_{ML}(X)\left[\frac{mg}{g}\right]*d_{ML}\,[m] + w_{PL}(X)\left[\frac{mg}{g}\right]*d_{PL}\,[m])}{100\,[cm]} \qquad \text{(eq. 1)}$$

https://doi.org/10.5194/essd-2022-123
Preprint. Discussion started: 1 July 2022


Open Access Earth System Science Data Discussions

3 Results

3.1 Geographical and lithological representation

Our sampling locations represent 13 out of 17 original geographic domains (missing: North Asia and North America, ice, none assigned), defined by the base map (76.5 %) (Table 1, Fig. S1 and Table S2) of the Arctic. The single areas and shares for the maps of Canada/Alaska, Greenland and North Europe/Russia are given in Table S3. Our data represent 17 eras of the Geological Map of the Arctic. The age ranged between 2.6 and 2,500 mya. The number of samples per age code are shown in Fig S2. Our data represent 14 lithological classes of the "Geological Map of the Arctic" (Table S4). These 14 lithological classes represent 7.63×1012 m² out of 1.57×1013 m² (48.49 % of the area represented by the Geological Map of the Arctic, including ice sheets). Sediments cover 1.03×1013 m² of the Arctic. Our data represent sedimentary classes that cover 6.77×1012 m² (65.9 % of the Arctic sediment cover) (Fig. S3). In total 3.68×1011 m² of 7.37×1011 m² (49.9 %) of Yedoma deposits were represented (Fig. S4). The 14 lithological classes can be observed in the igneous type (extrusive: mafic. class 1, n=26), type unclassified (Metamorphic undivided: class 2, n=21) and the sedimentary type (Carbonate: class 3, n=24; class 4, n=58; class 5, n=64; Clastic: shallow marine: class 6, n=13; Clastic: deltaic and nearshore: class 7, n=68; Sedimentary: undivided: class 8, n=38; class 9, n=39; Clastic: shallow marine: class 10, n=91; class 11, n=60; Sedimentary and/or volcanic: undivided: class 12, n=21; and Slope and deep water: class 13, n=43; class 14, n=8).

https://doi.org/10.5194/essd-2022-123
Preprint. Discussion started: 1 July 2022

Open Access Earth System Science Data Discussions

171 **Table 1**: First column lists original parameters given by the Geological Map of the Arctic (Harrison et al., 2011) and
172 Yedoma deposits (Strauss et al., 2021b). The column "Represented" gives absolute numbers for chronological or
173 lithological classes and of the area extrapolated by this study. For the area, relative share in comparison to total area
174 given by original studies is given, too.

Parameter	Represented	Explanation	Example
Geographic domain	13 (76.5%)	"Phanerozoic regions are based on major physiographic features of the Arctic" (Harrison et al., 2011)	Interior western Alaska
Era	17 (2.6 – 2,500 mya)	"Standardization of map-unit attributes has been facilitated by the International Stratigraphic Chart (August 2009 version) published by the International Commission on Stratigraphy (ICS)" (Harrison et al., 2011)	Neogene (23.0 - 2.6 Ma)
Represented area	7.63×10^{12} m² (43.03%)	Area of the Geological Map of the Arctic (Harrison et al., 2011) containing own data to element concentrations (Fig. 3-8).	
Lithological class	14	Specification and examples of rock type	Lithological class 2: Gneiss, migmatite; reworked amphibolite and granulite facies rocks
Sediments	6.77×10^{12} m² (65.9%)	Areas with lithological classes of the sedimentary type	Lithological class 7: Sandstone, siltstone, shale, coal; plant fossils; metamorphic grade not identified
Yedoma deposition	3.68×10^{11} m² (49.9%)	Areas that contain Yedoma deposits defined by Strauss et al. (2021b)	

175

https://doi.org/10.5194/essd-2022-123
Preprint. Discussion started: 1 July 2022

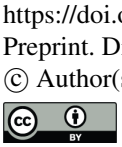

Open Access Earth System Science Data Discussions

176

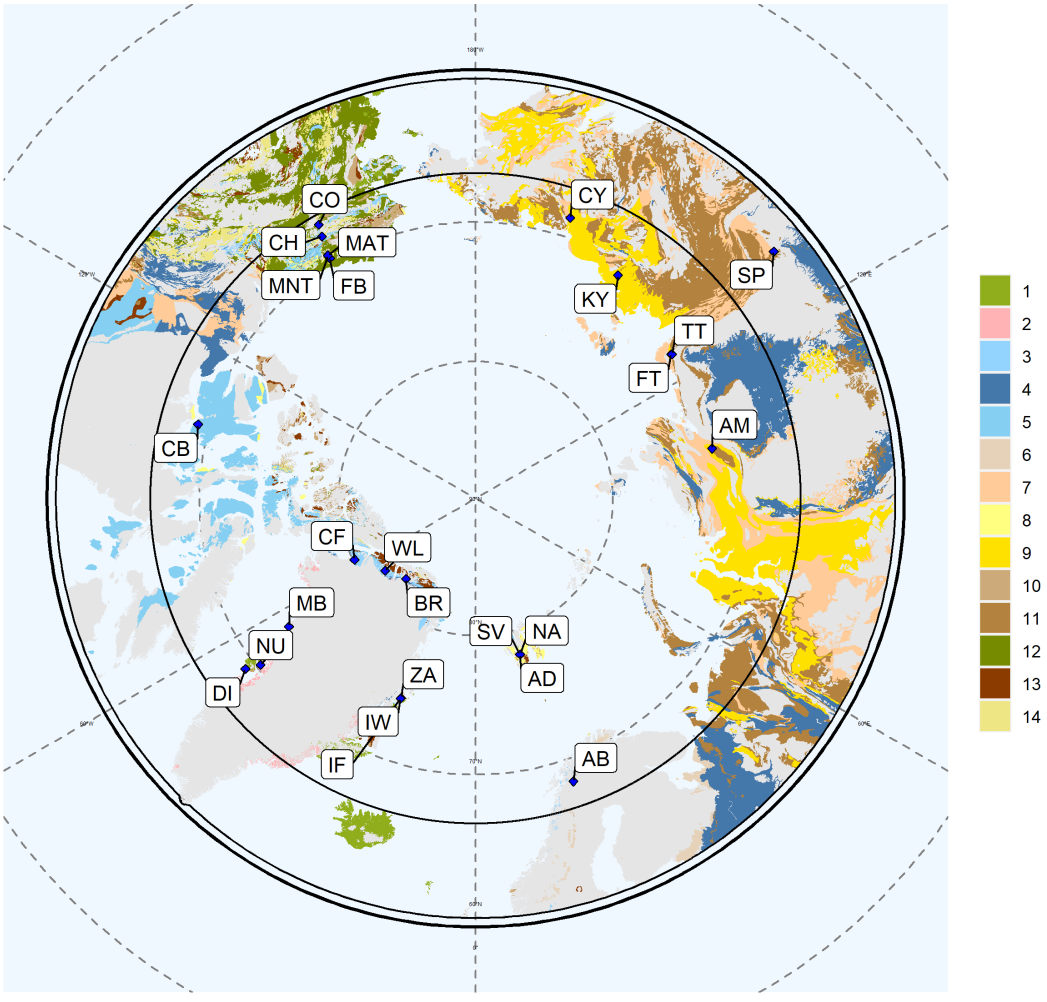

177

178

179 Fig. 1: Map of extrapolated element concentrations. The Arctic Circle (66.6°N) is included as a black circle. Each
180 color represents a bedrock lithology: 1: Basalt, olivine basalt, tholeiite, alkali basalt, basanite, pillow basalt, flood
181 basalt (n=26); 2: Gneiss, migmatite; reworked amphibolite and granulite facies rocks (n=11); 3: Limestone, dolostone,
182 shale, evaporites, chalk; carbonate reefs or metamorphosed equivalent (n=24); 4: Limestone, dolostone, shale,
183 evaporites, chalk; carbonate reefs; metamorphic grade not identified (n=58); 5: Limestone, dolostone, shale,
184 evaporites, chalk; carbonate reefs (n=64); 6: Quartz sandstone, siltstone, claystone, limestone, dolostone,
185 conglomerate, tillite (n=13); 7: Sandstone, siltstone, shale, coal; plant fossils; metamorphic grade not identified
186 (n=68); 8: Sandstone, siltstone, shale, limestone (n=38); 9: Sandstone, siltstone, shale, limestone; metamorphic grade

https://doi.org/10.5194/essd-2022-123
Preprint. Discussion started: 1 July 2022

not identified (n=39); 10: Sandstone, siltstone, shale; marine fossils (n=91); 11: Sandstone, siltstone, shale; marine fossils; metamorphic grade not identified (n=60); 12: Sedimentary and/or volcanic rock: undivided (n=21); 13: Shale, chert, iron-formation, greywacke, turbidite, argillaceous limestone, matrix-supported conglomerate (n=43); 14: Shale, chert, iron-formation, greywacke, turbidite, argillaceous limestone, matrix-supported conglomerate or metamorphosed equivalent (n=8). Grey color means areas of base map that are not represented by our data on element concentrations. Abbreviations for locations: CH: Alaska, Chandalar; CO: Alaska, Coldfoot; FB: Alaska, Franklin Bluff-Dry; MAT: Alaska, Moist acidic tundra; MNT: Alaska, Moist non-acidic tundra; CB: Canada, Cambridge Bay; BR: Greenland, Brønlund; CF: Greenland, Cass Fjord; DI: Greenland, Disko; MB: Greenland, Melville Bay; NU: Greenland, Nussuaq; WL: Greenland, Warming Land; ZA: Greenland, Zackenberg; IW: Greenland, Zackenberg, Ice Wedge; IF: Greenland, Zackenberg, Infilling Fan; AM: Russia, Ary-Mas; CY: Russia, Chersky; KY: Russia, Kytalyk; FT: Russia, Lena delta, first terrace; TT: Russia, Lena Delta, third terrace; SP: Russia, Spasskaya; AB: Sweden, Abisko; AD: Svalbard, Adventalen; NA: Svalbard, Adventalen; SV: Svalbard. This map is based on the Geological Map of the Arctic (Harrison et al., 2011).

https://doi.org/10.5194/essd-2022-123
Preprint. Discussion started: 1 July 2022

3.2 Element availabilities across lithological classes at 0-1 m depth

The lithological classes differed substantially in their element availabilities (Fig. 2; Fig S5):

- We found a large range in **ASi concentrations** in the Arctic covering values from 0.03±0 mg g^{-1} DW ASi to 6.68±1.17 mg g^{-1} DW ASi. The highest concentrations of ASi were found in basalt and associated rock (class 1: 6.68±1.17 mg g^{-1} DW ASi), Gneiss and associated rock (class 2: 4.11±1.24 mg g^{-1} DW ASi), Sandstone and associated rock (class 9: 2.01±0.24 mg g^{-1} DW ASi. class 10: 2.06±0.01 mg g^{-1} DW ASi). ASi concentrations were lowest in Limestone (class 3: 0.03±0 mg g^{-1} DW ASi) (Fig. 2).

- **Si concentrations** were highest in Limestone and associated rock including shale (class 4: 5.65±0.78 mg g^{-1} DW Si), Quartz sandstone (class 6: 6.61±1.83 mg g^{-1} DW Si) and Sandstone (class 7: 5.46±0.66 mg g^{-1} DW Si). Si concentrations were lowest in Limestone and associated rock (class 3: 0.1±0.02 mg g^{-1} DW Si) (Fig. 2).

- The highest **Ca concentrations** were observed in Limestone and associated rock (class 3: 10.73±2.15 mg g^{-1} DW Ca), Sedimentary and/or volcanic rock (class 12: 8.77±0.12 mg g^{-1} DW Ca) and Sandstone and associated rock (class 8: 8.06±0.36 mg g^{-1} DW Ca). Ca concentrations were lowest in Gneiss (class 2: 0.05±0.02 mg g^{-1} DW Ca) (Fig. 2).

- **Fe concentrations** were highest in shale and associated rock (class 13: 2.93±0.45 mg g^{-1} DW Fe), Limestone (class 4: 2.28±0.32 mg g^{-1} DW Fe) and Quartz sandstone (class 6: 2.49±0.69 mg g^{-1} DW Fe). The lowest Fe concentrations were observed in lithological Limestone and associated rock (class 3: 0.01±0.001 mg g^{-1} DW Fe) (Fig. 2).

- The highest **concentrations of Al** were observed in to quartz sandstone (class 6: 2.52±0.70 mg g^{-1} DW Al), Sandstone (class 7: 1.63±0.20 mg g^{-1} DW Al) and shale and associated rock (class 13: 1.5±0.23 mg g^{-1} DW Al). The lowest Al concentrations were observed in limestone and associated rock (class 3: 0.02±0 mg g^{-1} DW Al) (Fig. 2).

- High **P concentrations** were observed in limestone and associated rock (class 4: 0.31±0.04 mg g^{-1} DW P), Sandstone (class 7: 0.19±0.02 mg g^{-1} DW P) and Shale and associated rock (class 14: 0.15±0.05 mg g^{-1} DW P). P concentrations were lowest in Basalt and associated rock (class 1: 0.0116±0.002 mg g-1 DW P) (Fig. 2).

https://doi.org/10.5194/essd-2022-123
Preprint. Discussion started: 1 July 2022

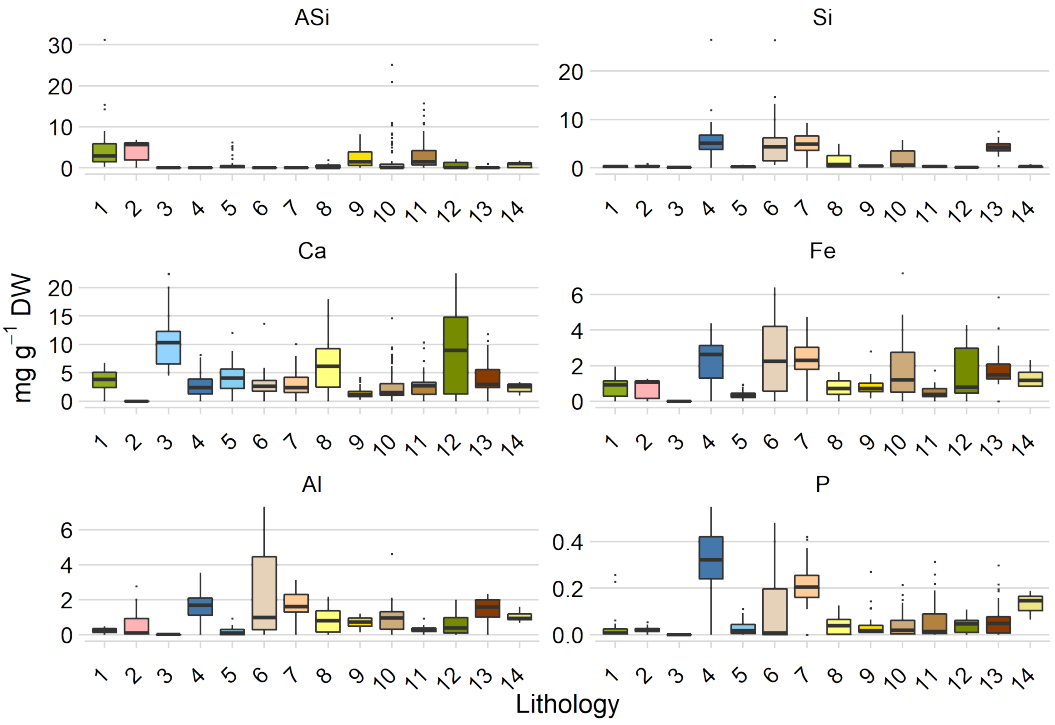

Fig. 2: Element concentrations related to lithology. Each color represents a bedrock lithology: 1: Basalt, olivine basalt, tholeiite, alkali basalt, basanite, pillow basalt, flood basalt (n=26); 2: Gneiss, migmatite; reworked amphibolite and granulite facies rocks (n=11); 3: Limestone, dolostone, shale, evaporites, chalk; carbonate reefs or metamorphosed equivalent (n=24); 4: Limestone, dolostone, shale, evaporites, chalk; carbonate reefs; metamorphic grade not identified (n=58); 5: Limestone, dolostone, shale, evaporites, chalk; carbonate reefs (n=64); 6: Quartz sandstone, siltstone, claystone, limestone, dolostone, conglomerate, tillite (n=13); 7: Sandstone, siltstone, shale, coal; plant fossils; metamorphic grade not identified (n=68); 8: Sandstone, siltstone, shale, limestone (n=38); 9: Sandstone, siltstone, shale, limestone; metamorphic grade not identified (n=39); 10: Sandstone, siltstone, shale; marine fossils (n=91); 11: Sandstone, siltstone, shale; marine fossils; metamorphic grade not identified (n=60); 12: Sedimentary and/or volcanic rock: undivided (n=21); 13: Shale, chert, iron-formation, greywacke, turbidite, argillaceous limestone, matrix-supported conglomerate (n=43); 14: Shale, chert, iron-formation, greywacke, turbidite, argillaceous limestone, matrix-supported conglomerate or metamorphosed equivalent (n=8). All values are given in mean and standard error. The distribution of the lithological classes is shown in Fig. 1, the assignment to the geographic domain is given in Table S5.

https://doi.org/10.5194/essd-2022-123
Preprint. Discussion started: 1 July 2022

3.3 Maps of element concentration in 1 m depth

3.3.1 Amorphous silica in top 1 m

We found the highest concentrations of ASi located in the Arctic-North Atlantic region (Fig. 3). Here, mafic basalt and metamorphic Gneiss are dominant (lithological class 1 and 2) and contained concentrations of 4.11±1.24 to 6.68±1.17 mg ASi g-1DW. Other high concentrations of ASi were found for the Brooks Range (Alaska), Chukotka, Arctic Shelf (eastern Siberia) and the West Siberian Basin. Those soil contained 2.01±0.24 mg ASi g-1 DW (lithological class 9). The Verkhoyansk-Kolyma region showed a lower concentration of 1.48±0.16 mg ASi g-1DW (lithological class 11). We found similar concentrations (1.24±0.14 mg ASi g-1DW; lithological class 5) were found for the Canadian Shield. We found low concentrations of 0.31±0.01 mg ASi g-1 DW (lithological class 12) in interior western Alaska and western parts of Brooks Range, Alaska, Chukotka and Arctic Shelf. Increasing active layer depth will potentially release higher ASi concentrations from permafrost soils (Fig. S6) in the Canadian Shield as the concentration in the permafrost layer is 2.80±2.50 mg ASi g-1DW (lithological class 5) compared to the 1.24±0.14 mg ASi g-1DW in the current active layer (Table S4). A further increase in ASi concentration can be expected for the Arctic, North-Atlantic region by permafrost thaw as the concentration is 8.68±2.51 mg ASi g-1DW in the permafrost layer compared to the 4.11±1.24 ASi g-1DW of the current active layer (lithological class 1) (Fig. S6 Table S4). However, the permafrost layer in Siberia contains lower concentrations of ASi (0.77±0.23 mg ASi g-1DW, lithological class 9 and 1.38±0.28 mg ASi g-1DW, lithological class 11) compared to the current active layer with 2.01±0.24 mg ASi g-1DW (lithological class 9) and 1.48±0.16 mg ASi g-1DW (lithological class 11) probably leading to lower overall ASi concentrations with proceeding thaw.

https://doi.org/10.5194/essd-2022-123
Preprint. Discussion started: 1 July 2022

Open Access Earth System Science Data Discussions

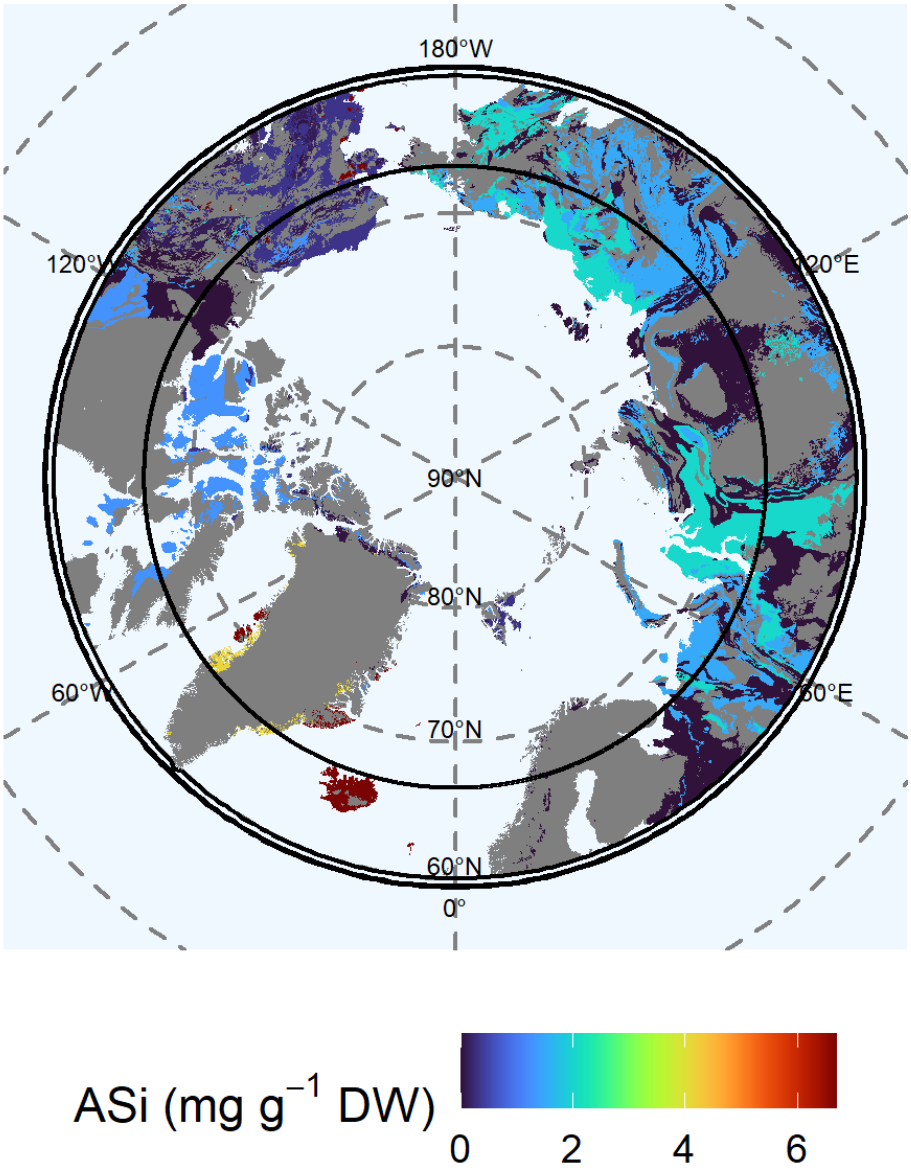

265

266 Fig. 3: Map of mean concentration of amorphous silica (ASi) in the top 100 cm of soils. For each lithological class
267 the mean concentration is shown. Grey shaded areas are not represented by our data.

https://doi.org/10.5194/essd-2022-123
Preprint. Discussion started: 1 July 2022

268 **3.3.2 Silicon in 0-1 m depth**

269 Available Si (Fig. 4) showed a different distribution than ASi (Fig. 3). High Si concentrations were generally
270 associated with sediments. We found high concentrations (5.65 ± 0.78 mg Si g-1 DW) for lithological class 4, the
271 West Siberian basin and the Siberian plain. Other regions with high Si concentrations were the East European plain,
272 the Ural Mountains and the Canadian Shield. Another lithological class with high Si concentrations (4.51 ±
273 0.69 mg Si g-1 DW) is class 13, located in the Innutian Region, North Greenland and in Alaska. In Alaska lithological
274 class 10 with moderate high concentrations of Si (2.06 ± 0.03 mg Si g-1 DW) is also abundant. We found low
275 concentration of Si (0.36 ± 0.05 mg Si g-1 DW, lithological class 9) for Brooks Range, Chukotka, Arctic shelf, the
276 West Siberia Basin and the Siberian Plain. In addition, the Verkhoyansk-Kolyma-Region and the East-European Plain
277 and the Ural Mountains were poor in Si (0.39 ± 0.04 mg Si g-1 DW, lithological class 11). Lowest concentrations
278 (0.15 ± 0.01 mg Si g-1 DW, lithological class 12) were observed in Interior Western Alaska. Increasing thawing depth
279 may potentially increase Si concentrations in the western Verkhoyansk-Kolyma-Region to the east European Platform
280 as the concentration in the permafrost layer is 6.26±1.52 mg Si g-1DW (lithological class 4) compared to the lower Si
281 concentration of the current active layer with 5.56±0.78 mg Si g-1DW (lithological class 4) (Figure S6, Table S4).
282

283

https://doi.org/10.5194/essd-2022-123
Preprint. Discussion started: 1 July 2022

Open Access Earth System Science Data Discussions

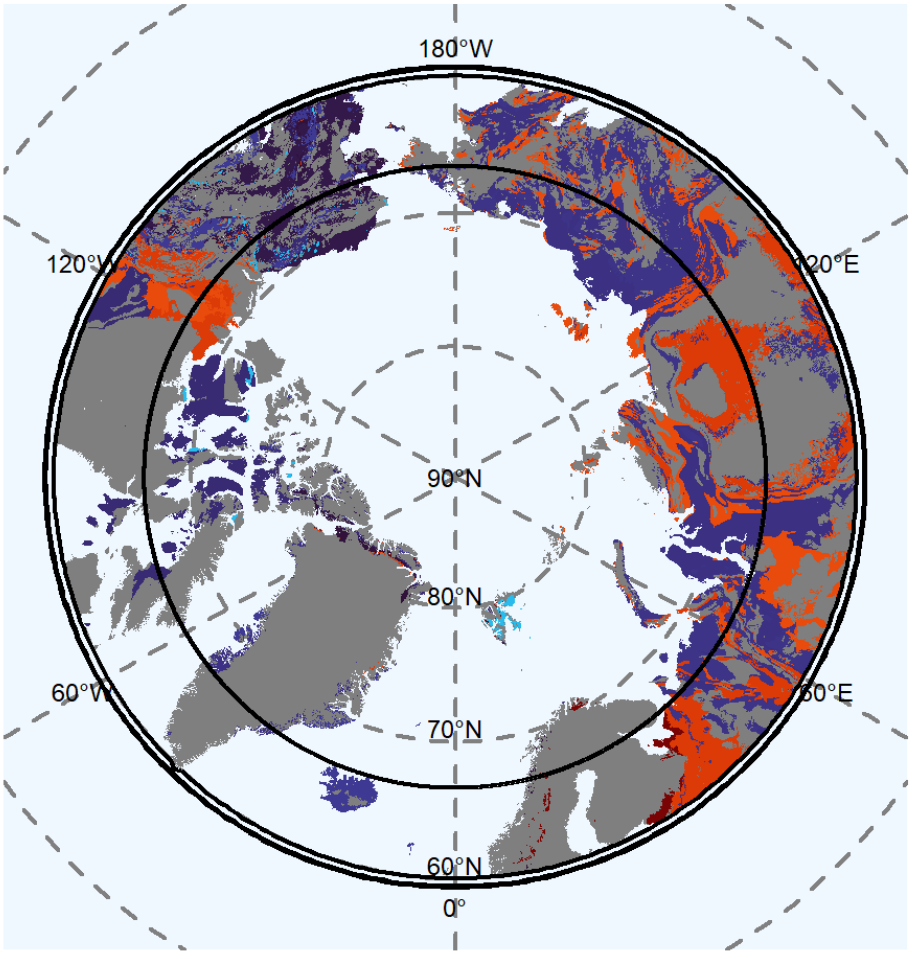

284

285 Fig. 4: Map of mean concentration of mineral silicon (Si) for the uppermost 100 cm of soils. For each lithological
286 class the mean concentration is shown. Blue colors represent low concentrations of Si; red colors represent high
287 concentrations. Grey shaded areas are not represented by our data.

https://doi.org/10.5194/essd-2022-123
Preprint. Discussion started: 1 July 2022


Open Access Earth System Science Data Discussions

288 **3.3.3 Calcium in 0-1m depth**

289 The highest Ca concentrations in soils was in limestone and associated rock (class 3: 10.73 ± 2.15 mg Ca g-1 DW) in
290 North Greenland, Alaska and the Canadian Shield (3.79 ± 0.45 mg Ca g-1 DW, lithological class 5) (Fig. 5). In
291 addition, supracrustal rocks in Alaska contained very high concentrations of Ca (8.77 ± 0.12 mg ca g-1 DW,
292 lithological class 12). Mafic rocks in the Arctic North Atlantic region (3.65 ± 0.70 mg Ca g-1 DW, lithological class
293 1) contained moderate Ca concentrations. We found moderate to low Ca concentrations (2.88 ± 0.32mg Ca g-1 DW,
294 lithological class 11) for the soils of the Verkhoyansk-Kolyma-Region, the East European Plain and the Ural
295 Mountains. Large regions of eastern and western Siberia and the Siberian Plain were poor in Ca (1.51 ± 0.14 mg Ca g-
296 1 DW, lithological class 9; 2.56 ± 0.34 mg Ca g-1 DW, lithological class 4). The Ca concentrations of the permafrost
297 layer for Alaska (10.42 ± 2.08 mg Ca g-1 DW, lithological class 12) is higher than in the active layer
298 (2.93±0.45 mg Ca g-1 DW) (Fig. S6). In the largest part of Siberia and the Canadian Shield the Ca concentrations are
299 slightly lower in the permafrost layer with 2.15 ± 0.96 mg Ca g-1 DW (lithological class 4) and 1.59 ± 0.32 mg Ca g-
300 1 DW, lithological class 7) than in the active layer with 2.56 ± 0.34 mg Ca g-1 DW (lithological class 4) and 1.51 ±
301 0.14 mg Ca g-1 DW, lithological class 7) (Figure S6, Table S4).

https://doi.org/10.5194/essd-2022-123
Preprint. Discussion started: 1 July 2022

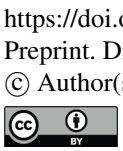

Open Access Earth System Science Data Discussions

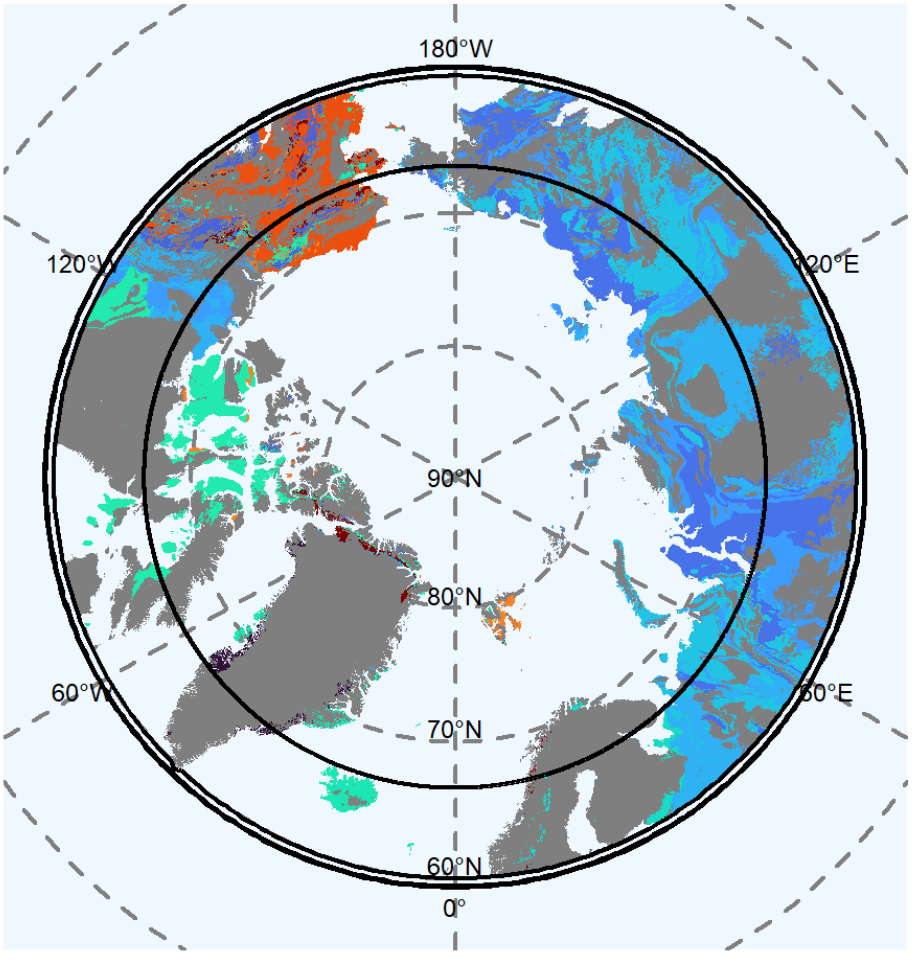

302

303 Fig. 5: Map of mean concentration of mineral calcium (Ca) for the uppermost 100 cm of soils. For each lithological
304 class the mean concentration is shown. Blue colors represent low concentrations of Ca, red colors represent high
305 concentrations. Grey shaded areas are not represented by our data.

306

https://doi.org/10.5194/essd-2022-123
Preprint. Discussion started: 1 July 2022


Open Access Earth System Science Data Discussions

307 **3.3.4 Iron (Fe) in 0-1 m depth**

308 Fe concentrations were higher in the eastern Arctic, than in the western Arctic (Fig. 6). We found highest
309 concentrations in northern Greenland (lithological class 13 contained 2.93 ± 0.45 mg Fe g-1 DW). The soils of the
310 lithological class 4 in the western Siberian Basin, Siberian and Canadian plain contained 2.28 ± 0.32 mg Fe g-1 DW.
311 The Verkhoyansk-Kolyma region showed similar Fe concentrations (2.21 ± 0.27 mg Fe g-1 DW, lithological class 7).
312 Moderate to high Fe concentration we found for igneous mafic rocks in Iceland and Greenland (0.94 ± 0.18 mg Fe g-
313 1 DW, lithological class 1) and for supracrustal rocks in Alaska (1.24 ± 0.14 mg Fe g-1 DW, lithological class 12).
314 The Chukotka region and western Siberia were relatively poor in Fe (0.83 ± 0.13 mg Fe g-1 DW, lithological class 9).
315 Eastern Siberia and North Europe contained even lower Fe concentrations (0.49 ± 0.04 mg Fe g-1 DW, lithological
316 class 11). Fe concentrations in the Canadian Shield were similarly low (0.41± 0.06 mg Fe g-1 DW, lithological class
317 12). We expect increasing Fe concentrations at the Canada and Greenland shield due to predicted future thaw of the
318 permafrost layer as the concentration in the permafrost layer (0.61± 0.15 mg Fe g-1 DW, lithological class 5) and in
319 parts of Alaska (1.97± 0.3 mg Fe g-1 DW, lithological class 14) is higher compared to the current active layer with
320 (0.41± 0.05 mg Fe g-1 DW, lithological class 5) and in parts of Alaska (1.08± 0.38 mg Fe g-1 DW, lithological class
321 14) (Fig. S7, Table S4).

https://doi.org/10.5194/essd-2022-123
Preprint. Discussion started: 1 July 2022

Open Access Earth System Science Data Discussions

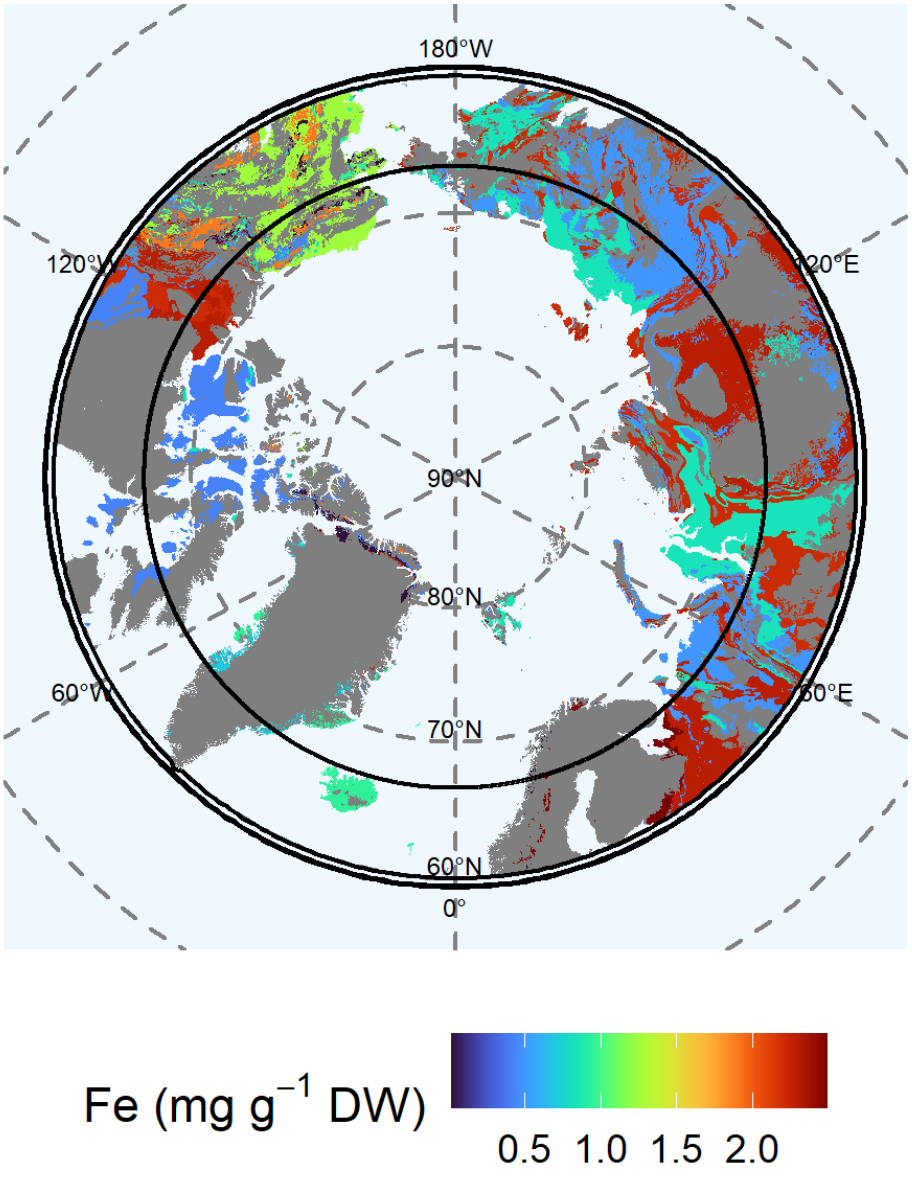

322

323 Fig. 6: Map of mean concentration of mineral iron (Fe) for the uppermost 100 cm of soils. For each lithological class
324 the mean concentration is shown. Blue colors represent low concentrations of Fe, red colors represent high
325 concentrations Grey shaded areas are not represented by our data.

https://doi.org/10.5194/essd-2022-123
Preprint. Discussion started: 1 July 2022

3.3.5 Aluminum in 0-1 m depth

Northern Europe contained highest concentrations of available Al (2.52 ± 0.07 mg Al g-1 DW, lithological class 6) (Fig. 7). Relative high concentrations of Al were distributed over Siberia and the Canadian Shield (1.63 ± 0.02 mg Al g-1 DW, lithological class 7; 1.57 ± 0.22 mg Al g-1 DW lithological class 4). Parts of Alaska contained moderate Al concentrations (0.94 ± 0.06 mg Al g-1 DW, lithological class 10; 1.5 ± 0.23 mg Al g-1 DW, lithological class 13), while areas represented by supracrustal rocks were poor in Al (0.47 ± 0.06 mg Al g-1 DW, lithological class 12). We found relative low concentrations (0.73 ± 0.01 mg g-1 DW) of Al for Chukotka, eastern and western Siberia observed in lithological class 9. The Verkhoyansk-Kolyma Region and the East European plain showed the lowest Al concentrations (0.26 ± 0.02 mg Al g-1 DW, lithological class 11), together with the Canada plain (0.21 ± 0.03 mg g-1 DW Al, lithological class 5). Increasing thawing depth may increase the Al concentration by the predicted thaw of the permafrost layer in North Europe as the concentration in the permafrost layer is 4.88± 1.02 mg Al g-1 DW (lithological class 6) and across the Greenland and Canadian shield it is 0.3± 0.07 mg Al g-1 DW (lithological class 5) compared to the current active layer with 2.52± 0.7 mg Al g-1 DW (lithological class 6) and across the Greenland and Canadian shield it is 0.21± 0.03 mg Al g-1 DW (lithological class 5) (Fig. S7, Table S4).

https://doi.org/10.5194/essd-2022-123
Preprint. Discussion started: 1 July 2022

Open Access Earth System Science Data Discussions

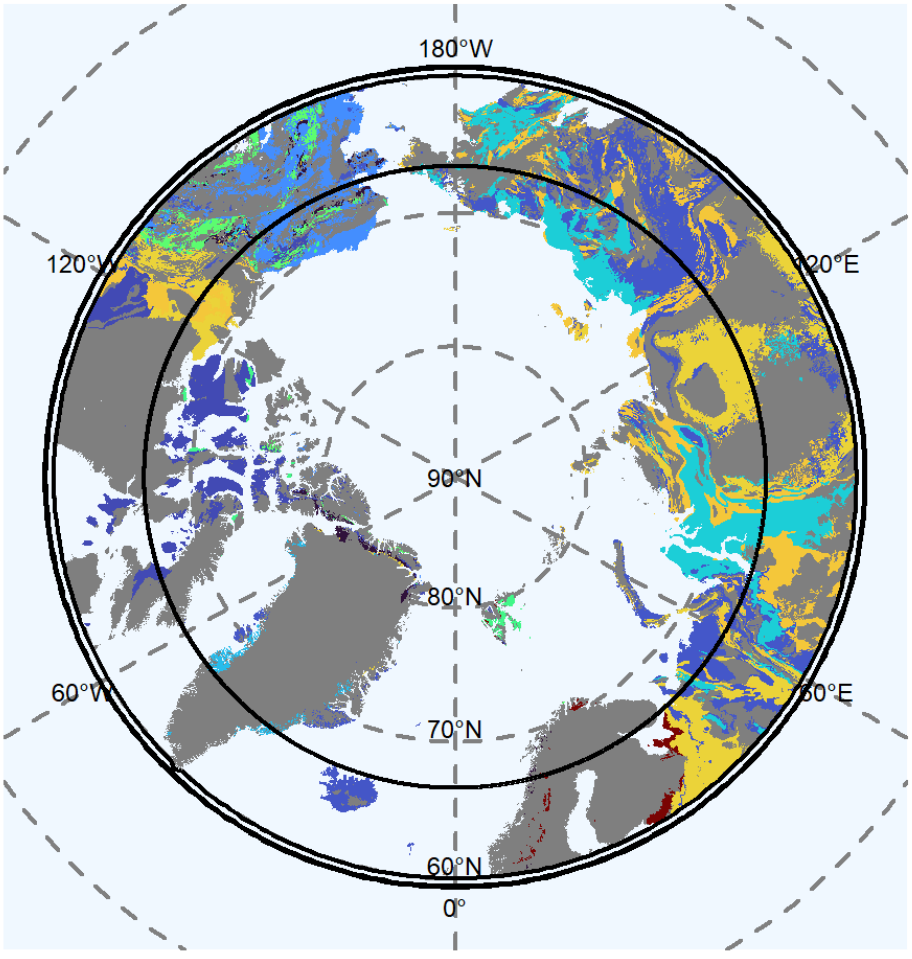

340

341 Fig. 7: Map of mean concentration of mineral aluminum (Al) for the uppermost 100 cm of soils. For each lithological
342 class the mean concentration is shown. Blue colors represent low concentrations of Al, red colors represent high
343 concentrations. Grey shaded areas are not represented by our data .

https://doi.org/10.5194/essd-2022-123
Preprint. Discussion started: 1 July 2022


Open Access Earth System Science Data Discussions

344 **3.3.6 Phosphorous in 0-1 m depth**

345 We found the highest P concentrations we found for the West Siberian Basin, the Canadian Shield and the Siberian
346 and East European Plain (0.306 ± 0.042 mg P g-1 DW, lithological class 4) (Fig. 8). In the Chukotka region the P
347 concentrations were 0.189 ± 0.023 mg P g-1 DW (lithological class 7. We found moderate P concentration for
348 Northern Europe (0.123 ± 0.034 mg P g-1 DW, lithological class 6) and in Alaska (0.153± 0.054 mg P g-1 DW,
349 lithological class 14). Wide areas of supracrustal rocks in Alaska were poor in P (0.024 ± 0.004 mg P g-1 DW,
350 lithological class 12). The Canadian shield (0.037 ± 0.005 mg P g-1 DW, lithological class 5), the Verkhoyansk-
351 Kolyma region, the east European Plain (0.017 ± 0.002 mg P g-1 DW, lithological class 11) and the Chukotka region
352 (0.030 ± 0.003 mg P g-1 DW, lithological class 9) were poor in P. Due to permafrost thaw we expect increasing P
353 concentrations the Canadian shield as the P concentrations in the permafrost layer is 0.06± 0.01 mg P g-1 DW
354 (lithological class 5) compared to the current active layer with 0.04± 0.005 mg P g-1 DW (lithological class 5) (Fig. 7,
355 Table S4).

https://doi.org/10.5194/essd-2022-123
Preprint. Discussion started: 1 July 2022

Open Access Earth System Science Data Discussions

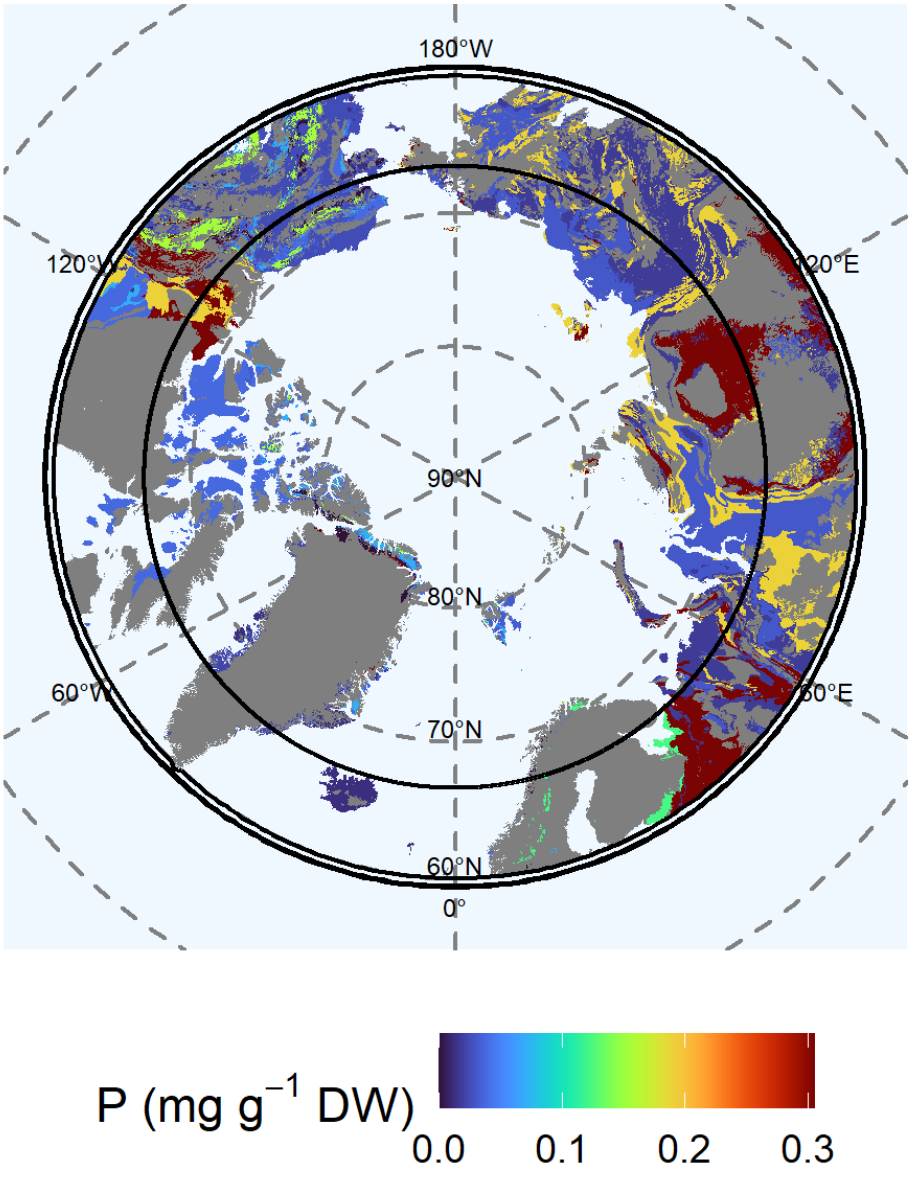

356

357 Fig. 8: Map of mean concentration of mineral phosphorous (P) for the uppermost 100 cm of soils. For each
358 lithological class the mean concentration is shown. Blue colors represent low concentrations of P, red colors
359 represent high concentrations. Grey shaded areas are not represented by our data .

https://doi.org/10.5194/essd-2022-123
Preprint. Discussion started: 1 July 2022

4 Discussion

4.1 Element availability in relation to lithology and geography

We found large differences in the availability of all analysed elements between the different lithology classes of the Arctic. The igneous lithological type for example is dominated by alkaline and Ca-rich basaltic rocks from Alaska. Rocks built up by sedimentation are often more complex or variable in their chemical composition than igneous rocks. Sedimentary rocks cover a wide range of pH, as the parent material is more diverse. Limestone sediments for example differ in their content of Fe and P, depending if their origin is biological (lithological class 4), physical or chemical. Sandstone can contain high Fe concentrations, too, but it contains Si as the main element (lithological class 7-8) (Yurchenko et al., 2019). Previously, there was no map existing for availability of Si, Ca, Fe, P, and Al in Arctic soils, and only a map on ASi stocks but not concentrations. Our maps show element concentration available for plants and microbes together. We further show what changes in element availability will occur during permafrost thaw and we discuss these changes in element availability in regard to occurring nutrient limitations and Arctic C-fluxes.

4.2 Relevance of element availability in a dynamic Arctic

Low temperatures in the Arctic systems slow down biological and chemical processes and preserve OM for millennia (Sher et al., 2005). Due to Arctic warming these processes are accelerated by an increased nutrient and OM mobilization from the permafrost (Salmon et al., 2016). Consequently, OM may become vulnerable to respiration (Hugelius et al., 2020; Strauss et al., 2017). However, OM is not the single driving force regarding the acceleration of Arctic soil respiration. Elements like Si, Ca, Fe, P and Al may also interfere this process (Monhonval et al., 2021a; Monhonval et al., 2021b).

Nutrient cycles and limitations were identified as important for improving of high latitude ecosystems estimations vegetation functional parameter like gross primary production (GPP) (Chadburn et al., 2017). The dataset presented in our study could therefore serve as a basis for providing soil nutrient concentrations for biogeochemical models that are capable of considering nutrient limitations in permafrost ecosystems. Our maps cover nearly the half of the Arctic area. The distribution of ASi in Arctic regions was first estimated by Alfredsson et al. (2016). Alfredsson et al. (2016) showed maps of ASi stocks (not concentrations) related to vegetation cover, covering 30 soil profiles. The effect of current vegetation on mineral availability in soils is low and associated with high uncertainties as the vegetation involved in forming the soil ASi pool may be different. A more appropriate measure of element availability may be parent material and lithology (Alloway, 2013). It was shown, that geochemical element concentration in Arctic permafrost soil allow to distinguish geologies (Reimann and Melezhik, 2001). Consequently, our lithology-based extrapolation of nutrient availability will help to reduce the so far uncertainties in pan-Arctic soil element availability. Due to deepening of the active layer, as for example observed at the Canadian shield and in the North-Atlantic region, our data suggest higher ASi concentrations, as the concentration in the permafrost layer is higher compared to shallower soil layers (Fig. S6). This may increase P and OM availability (Reithmaier et al., 2017; Schaller et al., 2019) by competing for binding sites on the surface of minerals subsequently mobilizing both P and OM, potentially increasing the leaching of both to the sea. It was also shown that Si leads to a release of P from minerals of Arctic

https://doi.org/10.5194/essd-2022-123
Preprint. Discussion started: 1 July 2022


Open Access Earth System Science Data Discussions

soils and increases OM decomposition, increasing soil greenhouse gas release (Schaller et al., 2019). Ca can immobilize OM by cation bridging and by this preserve OM from microbial decomposition (Sowers et al., 2020). Ca reduces the osmotic stress for microbes (Läuchli and Grattan, 2007) by decreasing the freezing point of water and increasing the availability of liquid pore water (Jessen et al., 2014). Ca is relevant for the mineral formation because it can bind CO2 as Ca(HCO3)2 in soil with pH higher than 7 (Dessert et al., 2003; Köhler et al., 2010). The concentration of soluble Ca in Yedoma soils is mainly driven by thermokarst processes. In deeper soil layers, Ca concentrations are usually lower than in upper layers. Consequently, a future increase in temperatures may lead to a widespread decrease in Ca concentrations, especially in the Yedoma regions. Fe is also of high importance for ecosystems as it is a key element in microbial activity (Colombo et al., 2014) and nitrogen fixation (Jasniewski et al., 2019). Fe minerals are important electron acceptors under anaerobic conditions and Fe is essential for microbial methane production (Colombo et al., 2018). After being released from rocks by weathering, Al forms amorphous aluminosilicates that mineralizes slowly (Schaller et al., 2021). Al is relevant for the OM respiration due to its high cytotoxicity to organisms (Rengel, 2004). Thawing permafrost may be a source for Al, especially across Canada, the Greenland shield and Northern Europe. Increasing P availability, as predicted for Greenland and the Canadian shield (Fig. 7) may for example increase CO2 release to the atmosphere by increasing the mineralization rates of OM (Street et al., 2018; Yang et al., 2021).

4.3 Importance of element interactions for nutrient availability

In permafrost layers, the mineralization of OM by microbial activity is negligible due to frozen conditions. Like in temperate soils, binding of OM on mineral phases can prevent OM from mineralization (Dutta et al., 2006; Mueller et al., 2015). Mineral phases may bind parts of soil OM reducing the amount of OM for microbial respiration. A large share of OM may be associated with iron and aluminium oxides/hydroxides. In particular iron minerals may strongly bind OM, whereby a high stability of stored carbon is likely (Herndon et al., 2017). Thereby the binding between OM and the minerals is determined by the quantity of minerals that can bind OM (Wiseman and Püttmann, 2006). This would imply that a higher concentration of Fe, Al and Ca in Arctic soils due to permafrost thaw may lead to a lower GHG emission from Arctic soils due to complexation of OM with those elements. Such increase in element availability binding OM and with this resulting in potentially lower GHG emissions may happen for Alaska (higher Ca and Fe concentration in permafrost layer compared to current active layer), Canadian Shield and Greenland (higher Fe and Al concentration in permafrost layer compared to current active layer), and North Europe (higher Al concentration in permafrost layer compared to current active layer) (see results part). However, lower Ca concentrations can be expected in large parts of Siberia and the Canadian Shield, as the concentrations in the permafrost layer are lower compared to the current active layer. Si however, can potentially mobilize OM from those phases, by binding competition of silicic acid with some functional groups of organic material (Hömberg et al., 2020), potentially increasing GHG emssions. An increase in Si availability upon permafrost thaw can be expected in the western Verkhoyansk-Kolyma-Region to the east European Platform as the concentration in the permafrost layer is higher compared to the current active layer (see results part). P competes with OM for binding on soil minerals (Schneider

https://doi.org/10.5194/essd-2022-123
Preprint. Discussion started: 1 July 2022

et al., 2010). Such increasing P concentration due to permafrost thaw can be expected for the Canadian Shield (results part). Based on the differences in element (Si, Fe, Al, Ca and P) concentration, the stability of OM differs in Arctic regions, depending on the dominating mineral composition, lithology and element availability. Also the availability of nutrients (P in this case) is modified by mineral composition. For example, P is often strongly bound to Fe mineral phases, reducing P availability (Gérard, 2016). Si however, is able to mobilize P from strong binding to Fe mineral by competing for binding sites (Schaller et al., 2019). Unlike Si, Ca binds P by calcium phosphate precipitation at alkaline conditions (Cao and Harris, 2008) or as calcium carbonate/phosphate co-precipitation (Otsuki and Wetzel, 1972). Under conditions of low Fe availability in soils, the binding of P may be related to Al-minerals (Eriksson et al., 2015). A lack of available P leads also to a reduction of the physiological activity of microbes (Walker et al., 2001), thus potentially reducing microbial respiration of OM. Free Si seems limit the availability of ions like Fe, Al, or Ca by precipitating those elements in amorphous or crystalline phases (Schaller et al., 2021). Hence, the mobilization of elements like Si, Ca, Fe and Al strongly interfere with both P and OM availability and thus potentially with GHG emissions. To unravel the dominant processes upon permafrost thaw, or which element mobilization is dominant in terms of OM binding or mobilization and with this affecting GHG emission, future studies are urgently needed.

4.4 Transport of elements to the Arctic Ocean

With the ongoing deepening of the active layer in Arctic soils, an increased leaching of elements and nutrients may occur (Mann et al., 2022; Sanders et al., 2022), which may substantially impact marine biodiversity and ecosystem function. We have shown for several regions of the Arctic that there will be regional differences in element mobilization upon permafrost thaw. For example, increased export of Fe and P, which are the main limiting nutrients for marine net primary production (NPP; Zabel and Schulz (2006)), has already contributed to a 30% increase in NPP in the Arctic Ocean between 1998 and 2009 (Arrigo and van Dijken, 2011). Increased Fe concentration upon permafrost thaw can be expected for the Canadian Shield, Greenland and Alaska, whereas increased P mobilization may occur only in the Canadian Shield. Si and Ca also have a crucial role in marine primary production. Both elements are components of the inorganic spheres of diatoms (Si) and coccolithophores (Ca), which fix CO2 in the Arctic Ocean, an important global carbon sink (Krause et al., 2018). At the Arctic Canadian coast, Si inputs led to an increase of diatoms from 2 % to 37 % (Terhaar et al., 2021). Diatoms and coccolithophores are the basis of the marine food chain, and therefore, shifts in their populations may have widespread implications for the marine ecosystem (Daniels et al., 2018). Permafrost thaw is likely to accelerate inputs of Si and Ca to Arctic waters. Increased Si concentration can be expected in the western Verkhoyansk-Kolyma-Region to the east European Platform as the concentration in the permafrost layer is higher compared to the current active layer, (see Results section). Ca mobilization may increase or decrease depending on the Arctic region. Increase Ca mobilization can be expected for Alaska, whereas a slight decrease in Ca mobilization may occur in large parts of Siberia and the Canadian Shield (see Results section). Yedoma deposits readily leach soluble ions, including Si and Ca, as a result of thaw degradation (Strauss et al., 2017). Alaskan soils store huge amounts of Ca in the mineral layer (see above) that could be transported to the Beringia Sea with increasing soil degradation, promoting the growth of coccolithophores. In Siberia, the Lena River could transport large

https://doi.org/10.5194/essd-2022-123
Preprint. Discussion started: 1 July 2022


Open Access Earth System Science Data Discussions

amounts of Si to the Laptev Sea increasing the growth of diatoms. The same could happen at the East European plain. In the same way P concentrations in these regions of the Arctic Sea could rise, too, as P concentrations in the permafrost layer of the Canadian Shield are higher compared with the current active layer (see results part). In summary, in the many areas of the Arctic with high Si, Ca and P storage, there could be increased inputs to Arctic waters with permafrost thaw potentially increasing CO2 fixation by marine primary production.

5 Data availability

The data for element availability from all single locations, soil profiles, transects, lithology's, as well as bootstrap data for location and lithology can be can be downloaded via the open-access MPG repository EDMONT under https://doi.org/10.17617/3.8KGQUN (Schaller and Göckede, 2022). During review process, the data is available under: https://edmond.mpdl.mpg.de/privateurl.xhtml?token=8cbb0bd8-790f-4719-8cd1-a3df4ff99477 (Schaller and Göckede, 2022) to allow corrections based on reviewer comments. The repository contains a readme file ("Read me.docx"). In this file, all necessary information can be found, including all columns descriptions need to use the data.
The element availability from all single locations, soil profiles, transects, lithology's labelled (loction_samples.txt) with following parameters: geological map of the Arctic, individual ID of the polygon, official name of the sampling site, study internal name of the soil sample, soil horizon, coordinates of sampling sites, concentration of alkaline extractable silicon, Mehlich-3 extractable Si, Ca, Fe Al and P, thickness of the layer, original depth where soil was taken, size of the polygon that contains the sampling site, age code, scientific name of the age, where bedrock was formed, scientific name of the eon, where bedrock was formed, scientific name of the era, where bedrock was formed, scientific name of the period, where bedrock was formed, maximal and minimal age of bedrock, information if lithogenesis was of the supracrustal, sedimentary or igneous type, most common rock types in the cluster group of the setting, code of metamorphic type, code of domain region, name of tectonic and geographic domain, as well as name of region within geographic domain.
In the location_bootstrap.txt file the bootstrapped means of concentration of alkaline extractable silicon, Mehlich-3 extractable Si, Ca, Fe Al and P for the organic, mineral active and permafrost layer of the single locations are given in mg/g DW.
In the file "lithology_bootstrap.txt" element concentration for the first 1 m, including organic, mineral and permafrost layer are given as bootstrapped mean with standard deviation for alkaline extractable silicon as well as Mehlich-3 extractable Si, Ca, Fe Al and P.

6 Conclusion

Here, we identified large differences in Si, Ca, Fe, P, and Al availability between different Arctic regions. With the future projected warming of the Arctic and the associated thaw of permafrost, the availabilities of the elements will change. Depending on dominance or limitation of certain elements, biogeochemical processes such as OM mineralization may increase or decrease. Moreover, not only microbial processes like OM respiration may be affected

https://doi.org/10.5194/essd-2022-123
Preprint. Discussion started: 1 July 2022

by changes in Si, Ca, Fe, P, and Al availability, but also processes such as primary production (CO2 fixation by plants) in terrestrial systems. This could be stabilizing soil OM, but may also trigger elevated biomass production of plants due to increased nutrient supply. In addition, marine systems will receive higher loads of leached elements, which could increase algae biomass production due to larger nutrient transport to the sea. Our spatially data product including the differences in elements availability between the different lithological classes and regions will help improving models of Arctic biogeochemical cycles for estimating future carbon feedback under the predicted climate change.

Competing interests. The contact author has declared that neither they nor their co-authors have any competing interests.

Acknowledgments. We thank Mrs. Lidia Völker (ZALF) for help with data extraction from the GIS polygons.

Financial support. The work was funded by the German Research Foundation (DFG), grant number SCHA 1822/12-1 to Jörg Schaller. J. Strauss work was embedded into the 'Changing Arctic Ocean (CAO)' program (CACOON project [#03F0806A (BMBF)]. Grant NSF-1417700 to SMN.

https://doi.org/10.5194/essd-2022-123
Preprint. Discussion started: 1 July 2022

519 **References**

520 Abbott, B. W., Jones, J. B., Godsey, S. E., Larouche, J. R., and Bowden, W. B.: Patterns and persistence of
521 hydrologic carbon and nutrient export from collapsing upland permafrost, Biogeosciences, 12, 3725-3740,
522 2015.
523 Alfredsson, H., Clymans, W., Hugelius, G., Kuhry, P., and Conley, D. J.: Estimated storage of amorphous silica
524 (ASi) in soils of the circum-Arctic tundra region, Glob. Biogeochem. Cycle, 30, 479–500, 2016.
525 Alloway, B. J.: Bioavailability of elements in soil. In: Essentials of medical geology, Springer, 2013.
526 Arrigo, K. R. and van Dijken, G. L.: Secular trends in Arctic Ocean net primary production, Journal of Geophysical
527 Research: Oceans, 116, 2011.
528 Box, J. E., Colgan, W. T., Christensen, T. R., Schmidt, N. M., Lund, M., Parmentier, F.-J. W., Brown, R., Bhatt, U.
529 S., Euskirchen, E. S., and Romanovsky, V. E.: Key indicators of Arctic climate change: 1971–2017, Environ.
530 Res. Lett., 14, 045010, 2019.
531 Brady, N. C. and Weil, R. R.: The nature and properties of soils, Prentice Hall Upper Saddle River, NJ, 2008.
532 Brown, J. and Romanovsky, V. E.: Report from the International Permafrost Association: State of permafrost in the
533 first decade of the 21st century, Permafrost and Periglacial Processess. 19 (2): 255-260, 2008. 2008.
534 Cao, X. and Harris, W.: Carbonate and magnesium interactive effect on calcium phosphate precipitation, Environ.
535 Sci. Technol., 42, 436-442, 2008.
536 Chadburn, S. E., Krinner, G., Porada, P., Bartsch, A., Beer, C., Belelli Marchesini, L., Boike, J., Ekici, A., Elberling,
537 B., and Friborg, T.: Carbon stocks and fluxes in the high latitudes: using site-level data to evaluate Earth
538 system models, Biogeosciences, 14, 5143-5169, 2017.
539 Colombo, C., Palumbo, G., He, J.-Z., Pinton, R., and Cesco, S.: Review on iron availability in soil: interaction of Fe
540 minerals, plants, and microbes, Journal of soils and sediments, 14, 538-548, 2014.
541 Colombo, N., Salerno, F., Gruber, S., Freppaz, M., Williams, M., Fratianni, S., and Giardino, M.: Impacts of
542 permafrost degradation on inorganic chemistry of surface fresh water, Global and Planetary change, 162, 69-
543 83, 2018.
544 Daniels, C. J., Poulton, A. J., Balch, W. M., Marañón, E., Adey, T., Bowler, B. C., Cermeño, P., Charalampopoulou,
545 A., Crawford, D. W., and Drapeau, D.: A global compilation of coccolithophore calcification rates, Earth
546 System Science Data, 10, 1859-1876, 2018.
547 DeMaster, D. J.: The supply and accumulation of silica in the marine environment, Geochim. Cosmochim. Acta, 45,
548 1715-1732, 1981.
549 Dessert, C., Dupré, B., Gaillardet, J., François, L. M., and Allegre, C. J.: Basalt weathering laws and the impact of
550 basalt weathering on the global carbon cycle, Chem. Geol., 202, 257-273, 2003.
551 Dutta, K., Schuur, E., Neff, J., and Zimov, S.: Potential carbon release from permafrost soils of Northeastern Siberia,
552 Glob. Change Biol., 12, 2336-2351, 2006.
553 Eriksson, A. K., Gustafsson, J. P., and Hesterberg, D.: Phosphorus speciation of clay fractions from long-term
554 fertility experiments in Sweden, Geoderma, 241, 68-74, 2015.

https://doi.org/10.5194/essd-2022-123
Preprint. Discussion started: 1 July 2022

555 Faucherre, S., Jørgensen, C. J., Blok, D., Weiss, N., Siewert, M. B., Bang-Andreasen, T., Hugelius, G., Kuhry, P.,
556 and Elberling, B.: Short and long-term controls on active layer and permafrost carbon turnover across the
557 Arctic, Biogeosciences, doi: 10.1002/2017JG004069, 2018. 2018.
558 Fuchs, M., Grosse, G., Strauss, J., Günther, F., Grigoriev, M., Maximov, G. M., and Hugelius, G.: Carbon and
559 nitrogen pools in thermokarst-affected permafrost landscapes in Arctic Siberia, Biogeosciences, 15, 953-971,
560 2018.
561 Gérard, F.: Clay minerals, iron/aluminum oxides, and their contribution to phosphate sorption in soils—A myth
562 revisited, Geoderma, 262, 213-226, 2016.
563 Harrison, C., St-Onge, M., Petrov, O., Strelnikov, S., Lopatin, B., Wilson, F., Tella, S., Paul, D., Lynds, T., and
564 Shokalsky, S.: A new geological map of the Arctic, 2011, 750-752.
565 Herndon, E., AlBashaireh, A., Singer, D., Chowdhury, T. R., Gu, B., and Graham, D.: Influence of iron redox
566 cycling on organo-mineral associations in Arctic tundra soil, Geochim. Cosmochim. Acta, 207, 210-231,
567 2017.
568 Holmes, R. M., Coe, M. T., Fiske, G. J., Gurtovaya, T., McClelland, J. W., Shiklomanov, A. I., Spencer, R. G.,
569 Tank, S. E., and Zhulidov, A. V.: Climate change impacts on the hydrology and biogeochemistry of Arctic
570 rivers, Climatic change and global warming of inland waters, 2013. 1-26, 2013.
571 Hömberg, A., Obst, M., Knorr, K.-H., Kalbitz, K., and Schaller, J.: Increased silicon concentration in fen peat leads
572 to a release of iron and phosphate and changes in the composition of dissolved organic matter, Geoderma,
573 374, 114422, 2020.
574 Hugelius, G., Loisel, J., Chadburn, S., Jackson, R. B., Jones, M., MacDonald, G., Marushchak, M., Olefeldt, D.,
575 Packalen, M., and Siewert, M. B.: Large stocks of peatland carbon and nitrogen are vulnerable to permafrost
576 thaw, Proceedings of the National Academy of Sciences, 117, 20438-20446, 2020.
577 Hugelius, G., Strauss, J., Zubrzycki, S., Harden, J. W., Schuur, E., Ping, C.-L., Schirrmeister, L., Grosse, G.,
578 Michaelson, G. J., and Koven, C. D.: Estimated stocks of circumpolar permafrost carbon with quantified
579 uncertainty ranges and identified data gaps, Biogeosciences, 11, 6573-6593, 2014.
580 IPCC: Climate Change 2021: The Physical Science Basis. Contribution of Working Group I to the Sixth Assessment
581 Report of the Intergovernmental Panel on Climate Change. Climate Change., 236 pp., 2021.
582 Jasniewski, A. J., Wilcoxen, J., Tanifuji, K., Hedman, B., Hodgson, K. O., Britt, R. D., Hu, Y., and Ribbe, M. W.:
583 Spectroscopic Characterization of an Eight-Iron Nitrogenase Cofactor Precursor that Lacks the “9th Sulfur”,
584 Angewandte Chemie, 131, 14845-14849, 2019.
585 Jessen, S., Holmslykke, H. D., Rasmussen, K., Richardt, N., and Holm, P. E.: Hydrology and pore water chemistry
586 in a permafrost wetland, Ilulissat, Greenland, Water resources research, 50, 4760-4774, 2014.
587 Kaiser, K. and Zech, W.: Competitive sorption of dissolved organic matter fractions to soils and related mineral
588 phases, Soil Sci. Soc. Am. J., 61, 64-69, 1997.
589 Köhler, P., Hartmann, J., and Wolf-Gladrow, D. A.: Geoengineering potential of artificially enhanced silicate
590 weathering of olivine, Proc. Natl. Acad. Sci. U. S. A., 107, 20228-20233, 2010.

https://doi.org/10.5194/essd-2022-123
Preprint. Discussion started: 1 July 2022

591 Krause, J. W., Duarte, C. M., Marquez, I. A., Assmy, P., Fernández-Méndez, M., Wiedmann, I., Wassmann, P.,
592 Kristiansen, S., and Agustí, S.: Biogenic silica production and diatom dynamics in the Svalbard region during
593 spring, Biogeosciences, 15, 6503-6517, 2018.
594 Kuhry, P., Bárta, J., Blok, D., Elberling, B., Faucherre, S., Hugelius, G., Jørgensen, C. J., Richter, A., Šantrůčková,
595 H., and Weiss, N.: Lability classification of soil organic matter in the northern permafrost region,
596 Biogeosciences, 17, 361-379, 2020.
597 Läuchli, A. and Grattan, S.: Plant growth and development under salinity stress. In: Advances in molecular breeding
598 toward drought and salt tolerant crops, Springer, 2007.
599 Mann, P. J., Strauss, J., Palmtag, J., Dowdy, K., Ogneva, O., Fuchs, M., Bedington, M., Torres, R., Polimene, L.,
600 and Overduin, P.: Degrading permafrost river catchments and their impact on Arctic Ocean nearshore
601 processes, Ambio, 51, 439-455, 2022.
602 Mishra, U., Hugelius, G., Shelef, E., Yang, Y., Strauss, J., Lupachev, A., Harden, J. W., Jastrow, J. D., Ping, C.-L.,
603 Riley, W. J., Schuur, E. A. G., Matamala, R., Siewert, M., Nave, L. E., Koven, C. D., Fuchs, M., Palmtag, J.,
604 Kuhry, P., Treat, C. C., Zubrzycki, S., Hoffman, F. M., Elberling, B., Camill, P., Veremeeva, A., and Orr, A.:
605 Spatial heterogeneity and environmental predictors of permafrost region soil organic carbon stocks, Science
606 Advances, 7, eaaz5236, 2021.
607 Monhonval, A., Mauclet, E., Pereira, B., Vandeuren, A., Strauss, J., Grosse, G., Schirrmeister, L., Fuchs, M., Kuhry,
608 P., and Opfergelt, S.: Mineral element stocks in the Yedoma domain: a novel method applied to ice-rich
609 permafrost regions, Frontiers in Earth Science, 9, 2021a.
610 Monhonval, A., Strauss, J., Mauclet, E., Hirst, C., Bemelmans, N., Grosse, G., Schirrmeister, L., Fuchs, M., and
611 Opfergelt, S.: Iron redistribution upon thermokarst processes in the Yedoma domain, Frontiers in Earth
612 Science, 9, 2021b.
613 Mueller, C. W., Rethemeyer, J., Kao-Kniffin, J., Löppmann, S., Hinkel, K. M., and G. Bockheim, J.: Large amounts
614 of labile organic carbon in permafrost soils of northern A laska, Glob. Change Biol., 21, 2804-2817, 2015.
615 Otsuki, A. and Wetzel, R. G.: Coprecipitation of phosphate with carbonates in a marl lake, Limnol. Oceanogr., 17,
616 763-767, 1972.
617 Quideau, S., Chadwick, O., Trumbore, S. E., Johnson-Maynard, J., Graham, R., and Anderson, M.: Vegetation
618 control on soil organic matter dynamics, Org. Geochem., 32, 247-252, 2001.
619 R_Core_Team: R: A language and environment for statistical computing, 2021. 2021.
620 Reimann, C. and Melezhik, V.: Metallogenic provinces, geochemical provinces and regional geology—what causes
621 large-scale patterns in low density geochemical maps of the C-horizon of podzols in Arctic Europe?, Appl.
622 Geochem., 16, 963-983, 2001.
623 Reithmaier, G. M. S., Knorr, K. H., Arnhold, S., Planer-Friedrich, B., and Schaller, J.: Enhanced silicon availability
624 leads to increased methane production, nutrient and toxicant mobility in peatlands, Scientific Reports, 7,
625 8728, 2017.
626 Rengel, Z.: Aluminium cycling in the soil-plant-animal-human continuum, Biometals, 17, 669-689, 2004.

https://doi.org/10.5194/essd-2022-123
Preprint. Discussion started: 1 July 2022

627 Romanovsky, V. E., Drozdov, D., Oberman, N. G., Malkova, G., Kholodov, A. L., Marchenko, S., Moskalenko, N.
628 G., Sergeev, D., Ukraintseva, N., and Abramov, A.: Thermal state of permafrost in Russia, Permafrost and
629 Periglacial Processes, 21, 136-155, 2010.
630 Salmon, V. G., Soucy, P., Mauritz, M., Celis, G., Natali, S. M., Mack, M. C., and Schuur, E. A.: Nitrogen
631 availability increases in a tundra ecosystem during five years of experimental permafrost thaw, Glob. Change
632 Biol., 22, 1927-1941, 2016.
633 Sanders, T., Fiencke, C., Fuchs, M., Haugk, C., Juhls, B., Mollenhauer, G., Ogneva, O., Overduin, P., Palmtag, J.,
634 and Povazhniy, V.: Seasonal nitrogen fluxes of the Lena River Delta, Ambio, 51, 423-438, 2022.
635 Schaller, J., Fauchere, S., Joss, H., Obst, M., Goeckede, M., Planer-Friedrich, B., Peiffer, S., Gilfedder, B., and
636 Elberling, B.: Silicon increases the phosphorus availability of Arctic soils, Scientific Reports, 9, 449, 2019.
637 Schaller, J. and Göckede, M., Pan-Arctic soil element availability estimations, doi:
638 https://doi.org/10.17617/3.8KGQUN, 2022.
639 Schaller, J., Puppe, D., Kaczorek, D., Ellerbrock, R., and Sommer, M.: Silicon Cycling in Soils Revisited, Plants,
640 10, 295, 2021.
641 Schirrmeister, L., Kunitsky, V., Grosse, G., Wetterich, S., Meyer, H., Schwamborn, G., Babiy, O., Derevyagin, A.,
642 and Siegert, C.: Sedimentary characteristics and origin of the Late Pleistocene Ice Complex on north-east
643 Siberian Arctic coastal lowlands and islands–A review, Quaternary international, 241, 3-25, 2011.
644 Schneider, M. P. W., Scheel, T., Mikutta, R., van Hees, P., Kaiser, K., and Kalbitz, K.: Sorptive stabilization of
645 organic matter by amorphous Al hydroxide, Geochim. Cosmochim. Acta, 74, 1606-1619, 2010.
646 Schuur, E., McGuire, A., Schädel, C., Grosse, G., Harden, J., Hayes, D., Hugelius, G., Koven, C., Kuhry, P.,
647 Lawrence, D., Natali, S., Olefeldt, D., Romanovsky, V., Schaefer, K., Turetsky, M., Treat, C., and Vonk, V.:
648 Climate change and the permafrost carbon feedback, Nature, 520, 171-179, 2015.
649 Schuur, E. A., Abbott, B., Bowden, W., Brovkin, V., Camill, P., Canadell, J., Chanton, J., Chapin, F., Christensen,
650 T., and Ciais, P.: Expert assessment of vulnerability of permafrost carbon to climate change, Climatic
651 Change, 119, 359-374, 2013.
652 Sher, A. V., Kuzmina, S. A., Kuznetsova, T. V., and Sulerzhitsky, L.: New insights into the Weichselian
653 environment and climate of the East Siberian Arctic, derived from fossil insects, plants, and mammals,
654 Quaternary science reviews, 24, 533-569, 2005.
655 Sims, J.: Comparison of Mehlich 1 and Mehlich 3 extractants for P, K, Ca, Mg, Mn, Cu and Zn in Atlantic coastal
656 plain soils, Commun. Soil Sci. Plant Anal., 20, 1707-1726, 1989.
657 Sowers, T. D., Wani, R. P., Coward, E. K., Fischel, M. H., Betts, A. R., Douglas, T. A., Duckworth, O. W., and
658 Sparks, D. L.: Spatially resolved organomineral interactions across a permafrost chronosequence, Environ.
659 Sci. Technol., 54, 2951-2960, 2020.
660 Strauss, J., Abbott, B. W., Hugelius, G., Schuur, E., Treat, C., Fuchs, M., Schädel, C., Ulrich, M., Turetsky, M., and
661 Keuschnig, M.: Permafrost, Recarbonizing global soils–A technical manual of recommended management
662 practices: Volume 2–Hot spots and bright spots of soil organic carbon, 2021a. 130, 2021a.

https://doi.org/10.5194/essd-2022-123
Preprint. Discussion started: 1 July 2022

663 Strauss, J., Laboor, S., Schirrmeister, L., Fedorov, A. N., Fortier, D., Froese, D., Fuchs, M., Günther, F., Grigoriev,
664 M., and Harden, J.: Circum-Arctic Map of the Yedoma permafrost domain, Frontiers in Earth Science,
665 2021b. 1001, 2021b.
666 Strauss, J., Schirrmeister, L., Grosse, G., Fortier, D., Hugelius, G., Knoblauch, C., Romanovsky, V., Schädel, C.,
667 von Deimling, T. S., and Schuur, E. A.: Deep Yedoma permafrost: A synthesis of depositional characteristics
668 and carbon vulnerability, Earth-Sci. Rev., 172, 75-86, 2017.
669 Strauss, J., Schirrmeister, L., Grosse, G., Wetterich, S., Ulrich, M., Herzschuh, U., and Hubberten, H. W.: The deep
670 permafrost carbon pool of the Yedoma region in Siberia and Alaska, Geophys. Res. Lett., 40, 6165-6170,
671 2013.
672 Street, L. E., Mielke, N., and Woodin, S. J.: Phosphorus availability determines the response of tundra ecosystem
673 carbon stocks to nitrogen enrichment, Ecosystems, 21, 1155-1167, 2018.
674 Terhaar, J., Lauerwald, R., Regnier, P., Gruber, N., and Bopp, L.: Around one third of current Arctic Ocean primary
675 production sustained by rivers and coastal erosion, Nat. Commun., 12, 1-10, 2021.
676 Tremblay, J.-É., Anderson, L. G., Matrai, P., Coupel, P., Bélanger, S., Michel, C., and Reigstad, M.: Global and
677 regional drivers of nutrient supply, primary production and CO_2 drawdown in the changing Arctic Ocean,
678 Progress in Oceanography, 139, 171-196, 2015.
679 Walker, D., Bockheim, J., Chapin Iii, F., Eugster, W., Nelson, F., and Ping, C.: Calcium-rich tundra, wildlife, and
680 the “Mammoth Steppe”, Quaternary Science Reviews, 20, 149-163, 2001.
681 Wiseman, C. and Püttmann, W.: Interactions between mineral phases in the preservation of soil organic matter,
682 Geoderma, 134, 109-118, 2006.
683 Yang, G., Peng, Y., Abbott, B. W., Biasi, C., Wei, B., Zhang, D., Wang, J., Yu, J., Li, F., and Wang, G.: Phosphorus
684 rather than nitrogen regulates ecosystem carbon dynamics after permafrost thaw, Glob. Change Biol., 27,
685 5818-5830, 2021.
686 Yurchenko, A. Y., Potapova, A., Bumagina, V., Vilesov, A., Chertina, K., Balushkina, N., Kalmykov, G., and
687 Khotylev, O.: Morphological and Lithogenetic Classification of the Carbonate Rocks of the Abalak–
688 Bazhenov Complex, Moscow University Geology Bulletin, 74, 372-379, 2019.
689 Zabel, M. and Schulz, H. D.: Marine geochemistry, Springer, 2006.

690